

---

# Use of a Custom-Made Patellar Groove Replacement in an American Staffordshire Terrier Puppy with a Severe Bone Defect in the Femoral Trochlea Caused by Hematogenous Osteomyelitis

---

Enrico Panichi , [Sara Sassaroli](#) <sup>\*</sup> , Giorgio Maria Ciccarese , [Valentina Riccio](#) , Caterina Balestriere , Marco Barbaccia , Fulvio Cappellari , Ekaterina Burkhan , [Angela Palumbo Piccionello](#)

Posted Date: 20 February 2024

doi: 10.20944/preprints202402.1172.v1

Keywords: osteomyelitis; custom-made patellar groove replacement; femoral trochlea; 3D-printing; patellar luxation; stifle joint; dog



Preprints.org is a free multidiscipline platform providing preprint service that is dedicated to making early versions of research outputs permanently available and citable. Preprints posted at Preprints.org appear in Web of Science, Crossref, Google Scholar, Scilit, Europe PMC.

Copyright: This is an open access article distributed under the Creative Commons Attribution License which permits unrestricted use, distribution, and reproduction in any medium, provided the original work is properly cited.

Disclaimer/Publisher's Note: The statements, opinions, and data contained in all publications are solely those of the individual author(s) and contributor(s) and not of MDPI and/or the editor(s). MDPI and/or the editor(s) disclaim responsibility for any injury to people or property resulting from any ideas, methods, instructions, or products referred to in the content.

Case Report

# Use of a Custom-Made Patellar Groove Replacement in an American Staffordshire Terrier Puppy with a Severe Bone Defect in the Femoral Trochlea Caused by Hematogenous Osteomyelitis

Enrico Panichi <sup>1</sup>, Sara Sassaroli <sup>2,\*</sup>, Giorgio Maria Ciccarese <sup>1</sup>, Valentina Riccio <sup>2</sup>, Caterina Balestriere <sup>1</sup>, Marco Barbaccia <sup>1</sup>, Fulvio Cappellari <sup>1</sup>, Ekaterina Burkhan <sup>3</sup> and Angela Palumbo Piccionello <sup>2</sup>

<sup>1</sup> Centro Traumatologico Ortopedico Veterinario, Via C. Festa 9, 16011 Arenzano, GE, Italy;

enricopanichi76@gmail.com (E.P.); ciccaresegiorgio@gmail.com (G.M.C.);

caterinabalestriere@gmail.com (C.B.); m.barbaccia89@gmail.com (M.B.); fulvio.cappellari@ctovet.com (F.C.)

<sup>2</sup> School of Biosciences and Veterinary Medicine, University of Camerino, Via Circonvallazione 93/95, 62024

Matelica, MC, Italy; valentina.riccio.dvm@gmail.com (V.R.); angela.palumbo@unicam.it (A.P.P.)

<sup>3</sup> Bonabyte, Begovoy proezd 7, Moscow, Russia; k.burkhan@bonabyte.net (E.B.)

\* Correspondence: sara.sassaroli@unicam.it; Tel.: Tel.: +39-0737-403403

**Simple Summary:** Osteomyelitis is an infection condition of the bone causing progressive inflammation which leads to bone lysis, periosteal reactions and ischemic regions of infected necrotic and devitalized tissue. It is necessary immediate and aggressive treatment with a prolonged antibiotic therapy, an abundant lavage of the affected region and several revision surgeries to debride infected and necrotic bone. The treatment of extensive bone defects and functional damage may require the use of prosthetic surgery, allowing the anatomical and functional recover of the affected area, and in some cases, it is necessary the use of customized prosthesis for a better anatomical and functional adaptation. In veterinary medicine, the implementation of 3D-printing technologies and the application of custom-made surgical implants and prosthetics have enabled the management of intricate orthopedic conditions that were previously only addressed through salvage procedures, such as arthrodesis or amputations. The purpose of this report is to describe the surgical technique and outcome of a custom-made patellar groove replacement in a puppy with a severe bone defect in the femoral trochlea caused by hematogenous osteomyelitis. This surgery showed excellent short-, medium- and long-term outcomes and it is the first report on custom-made patellar groove replacement available in the literature.

**Abstract:** An 8-months old male American Staffordshire terrier was referred for a no weightbearing lameness of the right pelvic limb, hyperthermia, lethargy and inappetence caused by hematogenous osteomyelitis. Orthopedic, radiographic and tomographic examinations revealed a bone sequestrum of 4 x 1.4 cm and active periosteal reaction of the caudo-lateral cortical in the metaphysis and the distal third of the right femoral diaphysis, medullary osteolysis and interruption of the cranio-medial cortical profile, with involvement of the femoral trochlea leading to a secondary medial patella luxation. Once skeletally mature, after 4 months from surgical debridement and aggressive antibiotic therapy against *Klebsiella oxytoca* revealed by bacteriological exam, the patient underwent prosthetic surgery for the application of a custom-made patellar groove replacement (PGR) to fill the bone defect and restore the femoral trochlea surface. Despite the serious injury that afflicted the right pelvic limb, the surgery had satisfactory outcomes until the last 18-months postoperative follow up.

**Keywords:** osteomyelitis; custom-made patellar groove replacement; femoral trochlea; 3D-printing; patellar luxation; stifle joint; dog

## 1. Introduction

Osteomyelitis is an inflammatory condition of the bone and bone marrow caused by an infectious agent such as bacteria, virus or fungi [1,2]. Osteomyelitis has been classified based on the pathway through which the infectious agent enters the site of infection: hematogenous and post-traumatic or direct inoculation [1]. Despite bones are naturally resistant to colonization and infection in physiologic conditions, the post-traumatic osteomyelitis, the most common source of osteomyelitis in dogs and cats, can develop as a result of a penetrating wound (e.g. foreign body or bite wound) or the introduction of foreign material (e.g. implants or prosthesis) [3–6]. A less common condition, it is the hematogenous osteomyelitis, that usually affected young animals and animals with abnormal immune systems, and results from the spread of bacteria, localized to a distant site, to bone via the bloodstream. Due to anatomic differences in the macro- and microcirculation (capillaries with an incomplete basement membrane and gaps between endothelial cells, and a sluggish blood flow within the metaphyseal capillaries), it most commonly affects the metaphyseal regions of long bones [1,6–9].

A patient suffering from osteomyelitis on a bone segment of a limb usually shows lameness on the affected limb, localized soft tissue swelling and painful. Muscle atrophy and draining tracts may be present. In addition, the affected animals are often systematically ill and clinical signs can include fever, inappetence and lethargy. Bone resorption, bone lysis, periosteal reactions and ischemic regions of infected necrotic and devitalized tissue can be detected. In case of osteomyelitis, it's necessary an immediate and aggressive therapy [1,10].

The resolutive treatment of osteomyelitis sometimes requires a long hospital recovery, a prolonged antibiotic therapy, an abundant lavage of the affected region and several revision surgeries to debride infected and necrotic bone [6,11]. The bone loss and significant functional defects may lead to a high risk of a delay healing time and recurrence of infection [6].

The treatment of extensive bone defects and functional damage may require the use of prosthetic surgery, allowing the anatomical and functional recover of the affected area [12]. Similar to human medicine, the veterinary field also offers a range of standard-sized joint prostheses that are readily available on the market. Total hip replacement (THR), total knee replacement (TKR), patellar groove replacement (PGR) and total elbow replacement (TER), but also compartmental prostheses such as biomechanically anatomic non-constrained compartmental partial elbow replacement (BANC PER), are some of the prostheses available [13–16]. Despite the different prosthetic models and size, in some cases it is necessary the use of customized prosthesis with specific characteristics for a better anatomical and functional adaptation [12,17,18]. In the last few years, in the realm of human and veterinary orthopedics, the utilization of 3D printing has surfaced as a valuable method for fabricating bespoke implants tailored to the precise requirements of recipients [12,17]. In veterinary medicine, the application of custom-made surgical implants and prosthetics has proven indispensable for addressing intricate orthopedic conditions and revision surgeries, such as nonunion or malunion fractures, tumors, bone deformities, severe traumatic injuries and substantial bone loss [12].

The objective of this case report is to describe the surgical technique and outcome of a custom-made PGR in an American Staffordshire terrier puppy with a severe bone defect in the femoral trochlea caused by hematogenous osteomyelitis. In our knowledge, this is first report on custom-made PGR available in the literature.

## 2. Case Report

An 8 months American Staffordshire terrier weighing 25 kg was referred to the Orthopedic Veterinary Trauma Center (Arenzano, Italy) for a no weightbearing lameness of the right hind limb. The lameness has suddenly arisen two weeks earlier without any traumatic episode and a progressive worsened. During this period, the owner reported that the dog presented recurrent and intermittent hyperthermia. Two months before, an endocarditis was diagnosed to the patient and treated with antibiotic therapy in another veterinary hospital.

The rectal temperature was increased (40.5°C). The patient manifested lethargy, inappetence and anorexia. A complete blood count and the serum biochemical profile revealed leukocytosis (27.10 x 10<sup>9</sup>/L; reference range: 6.00 – 17.00 x 10<sup>9</sup>/L) and an increment of total serum protein (8.3 g/dL; reference range: 5.2 – 8.2 g/gL) and hyperglobulinemia (5.2 g/dL; reference range: 2.5 – 4.5 g/gL).

The orthopedic examination revealed no weightbearing lameness (grade IV on scale from 0 to IV) [18] and severely edema of the right hind limb, pain on manipulation of the right stifle, joint swelling and grade III medial patellar luxation (MPL) [19] (Figure 1, Video S1). Caudo-cranial and medio-lateral radiographic projections of the right femur, performed by reference colleagues, highlighted an extensive periosteal reaction of the diaphysis and femoral metaphysis, and a radiolucent area in the distal metaphysis (Figure 2).



**Figure 1.** The 8 months American Staffordshire terrier referred to the Orthopaedic Veterinary Trauma Center (Arenzano, Italy) for a no weightbearing lameness of the right hind limb.

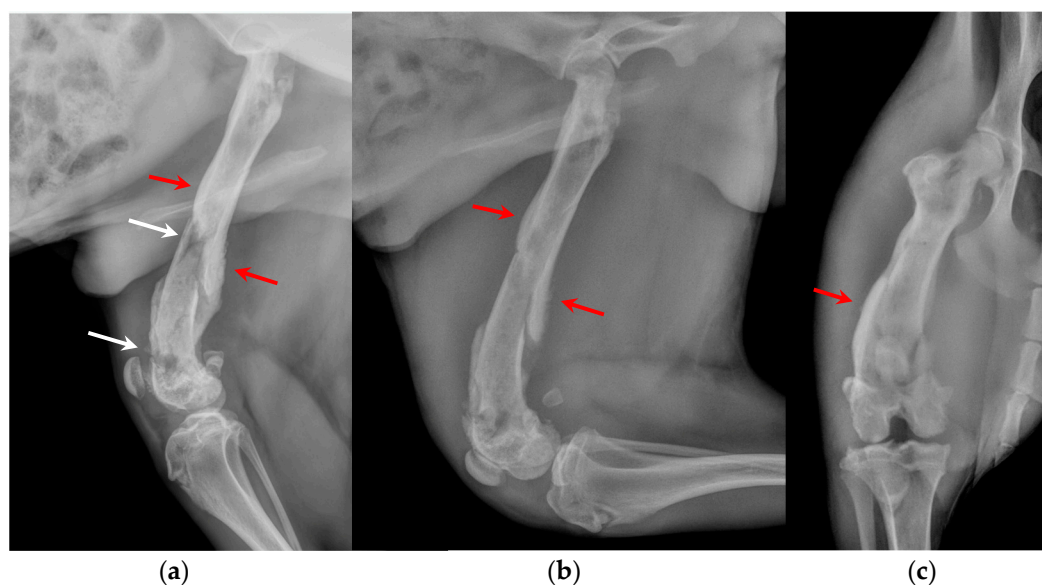


**Figure 2.** (a) Extended medio-lateral, (b) flexed medio-lateral and (c) cranio-caudal radiographic projections of the right stifle joint and femoral diaphysis, performed by reference colleagues, highlighted an extensive periosteal reaction of the diaphysis and femoral metaphysis (red arrows), and a radiolucent area (white arrows) in the distal metaphysis. Under anesthesia, a computed tomography study (CT; Somatom Emotion 16, Siemens, Germany) of the hind limbs was performed.

Under anesthesia, a computed tomography study (CT; Somatom Emotion 16, Siemens, Germany) of the hind limbs was performed. The tomographic images revealed medullary osteolysis of the metaphysis and the distal-middle third of the femoral diaphysis. In the metaphysis and the distal third of the femoral diaphysis a bone sequestrum was found: a wide interruption of the cranio-medial cortical profile, with involvement of the femoral trochlea, was observed with corticomedullary

fragment of 4 x 1.4 cm (length x width) medially dislocated at the level of the medullary cavity; the fragment was surrounded by a large hypodense halo. Secondary MPL and widespread subcutaneous and perifascial abscess lesion were also reported (Figure 3).



**Figure 3.** (a) Sagittal, frontal and transverse tomographic images of the metaphysis and the distal-middle third of the femoral diaphysis revealed medullary osteolysis, a wide interruption of the cranio-medial cortical profile with corticomedullary fragment of 4 x 1.4 cm (length x width) medially dislocated at the level of the medullary cavity (bone sequestrum), and an extensive periosteal reaction of caudo-lateral cortex of the femoral distal diaphysis. (b) A widespread subcutaneous and perifascial abscess lesion were also reported (white arrow).

The patient was subsequently subjected to arthrocentesis for bacteriological and cytological examination of synovial fluid. It appeared cloudy and similar-purulent at the macroscopic vision. During the same session, a joint irrigation with a sterile physiological solution was performed as previously reported [20].

Based on the anamnestic and clinical data, on radiographic and tomographic examination and on macroscopic appearance of synovial fluid, the diagnostic suspicion was septic arthritis of the right stifle joint and osteomyelitis of right distal femur.

Consequently, the patient was hospitalized in order to provide intravenous (IV) broad-spectrum antibiotic therapy (amoxicillin and clavulanic acid 20 mg/kg IV twice daily), anti-inflammatory therapy (meloxicam 0,1 mg/kg SC once a day) and maintenance fluid therapy (ringer's lactate 2 ml/kg/h IV), pending the results of bacteriological and cytologic examination.

After 5 days, the results of cytology and bacteriological exams of the synovial fluid showed a severe inflammatory process and the presence of *Klebsiella oxytoca*, a bacterium multidrug resistant sensitive to the antibiotic nitrofurantoin. These results and the images obtained from tomographic scans confirmed the diagnosis of osteomyelitis and septic arthritis.

In agreement with the owner, a surgical procedure was performed in order to remove the bone sequestrum, debride necrotic tissues and perform a copious lavage of the affected region (Figure 4). A modified Robert Jones splint was applied for 48 hours after the surgery. The patient was hospitalized for 48 hours and then discharged with a specific antibiotic therapy (nitrofurantoin 4 mg/kg PO twice daily) and anti-inflammatory therapy (meloxicam 0.1 mg/kg PO once daily). The antibiotic and anti-inflammatory therapy was prescribed and administered to the patient for 30 days once the patient was discharged.

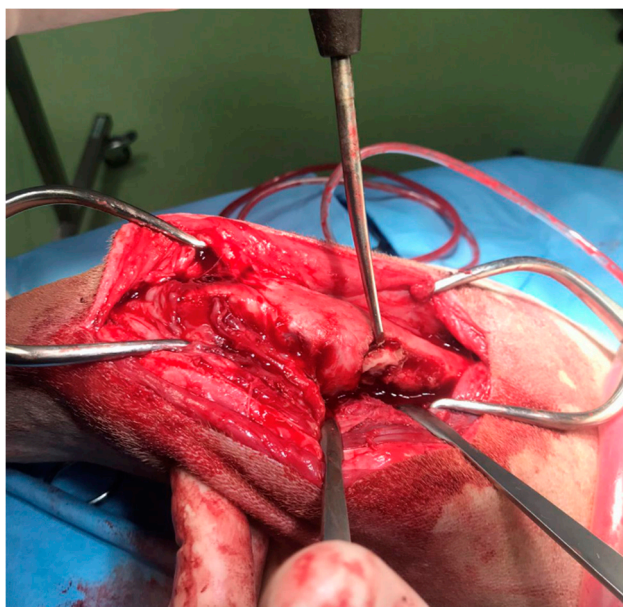


**Figure 4.** The intraoperative image of the bone sequestrum and of surgical debridement of the necrotic tissue.

At 12 months of age, once skeletally mature, the patient was again subjected to an orthopedic and radiographic evaluation and CT scans of the pelvis and the hind limbs. Orthopedic examination revealed a grade III of lameness (on scale from 0 to IV) [21], significant muscle hypotrophy, pain on manipulation of the right stifle, joint swelling and grade III MPL [19]. The severely edema of the limb observed during the first orthopedic evaluation disappeared (Video S2).

The CT showed an extensive bone defect on the metaphysis and on the distal third of the femoral diaphysis, with loss of the cranio-medial cortical of the distal femur and of the femoral trochlea and resulting medial patella luxation of the right hind limb. A three-dimensional (3D) reconstruction of the hind limbs was performed in order to evaluate their alignment and to design a custom-made PGR: a custom-made implant that fills the bone gap and allows to restore the articular surface of the missing femoral trochlea.

The measurements performed did not show significant deformity and different alignment between the pathological right hind limb and the contralateral in the frontal, sagittal and axial planes (Figure 5). Once the correct alignment was verified, a custom-made PGR and an osteotomy guide were planned using BonaPlanner computer-aided design CAD software (Bonabyte LLC, Moscow) in order to perform a prosthetic surgery to restore the articular surface of the femoral trochlea and resolve the bone defect.

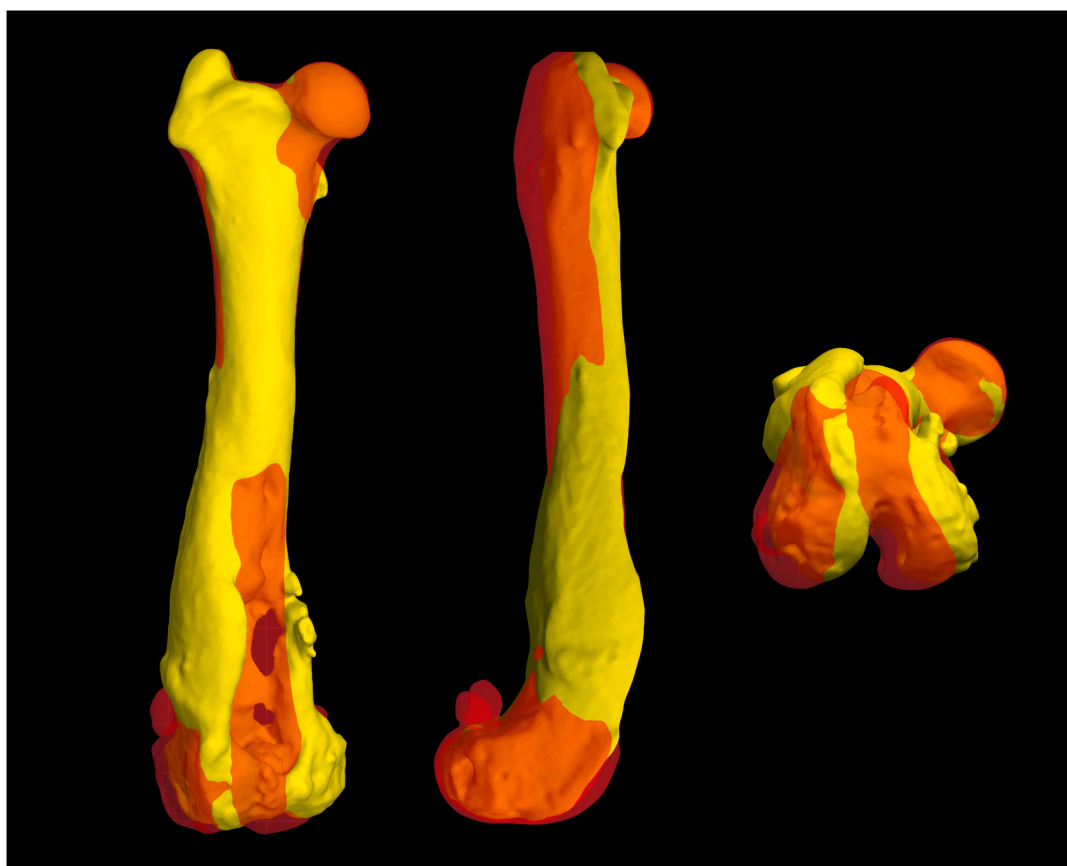


**Figure 5.** The superimposition of normal and pathological femur measurements obtained using BonaPlanner computer-aided design CAD software (Bonabyte LLC, Moscow) did not show significant deformity and different alignment between the pathological right hind limb and the contralateral hind limb in the frontal, sagittal and axial planes.

### 2.1. Planning of the osteotomy guide

An osteotomy guide was created to prepare the site of the prosthetic implant. The guide was designed in order to reproduce the osteotomy proposed by Dokic et al. for the removal of the femoral trochlear for application of Kyon® PGR [16]. The authors suggested to perform an osteotomy from the level of the origin of the tendon of the long digital extensor muscle (extensor digitorum pedis longus, EDPL) to the proximal end of trochlea [16]. The osteotomy guide accurately matched the cranial surface of the distal femoral epiphysis, in particular the partially intact lateral trochlear ridge, which represented an important and easily recognizable landmark during surgery for the correct application of the osteotomy guide on the bone. In the guide, there were four holes that allowed the insertion of four 2.0 mm Steinmann pins in order to fix the guide to the bone during osteotomy execution, and two slots, laterally and medially, that permitted entry and exit of a saw blade 1 mm thick (DePuy Synthes®). The four holes for pins application were designed to match the holes for the screws of the custom-made implant. The osteotomy guide was made of Nextdent SG (Surgical Guide) by 3D SYSTEM® and printed with a 3D printing machine (Form 2, formlabs®).

### 2.2. Planning of the custom trochlear prosthesis

The custom-made PGR prosthesis was made of titanium Ti-6Al-4V extra low interstitial (ELI) (grade 23) and was printed with a GE® M2 Series 5 laser. The prosthesis was designed in order to fill the bone defect and anatomically reproduce the shape of the femoral trochlea on the upper face of the implant. The mirror surface of the prosthesis that reproduce the femoral trochlea was made by polishing with diamond base abrasive material made by hand to reduce the coefficient of friction, similar to the prosthetic component of Kyon® PGR. [16] The portion of the prosthesis designed to fill

the bone defect had a porous structure with a cell size of 0,7-1 mm to promote the bone growth and osseointegration. The custom-made PGR prosthesis was secured to the bone with four locking screws (2.7 mm, Ti-6Al-4V ELI). The four holes for screws were designed one laterally and one medially the distal margin of the lateral and medial trochlear ridges, respectively; one laterally the proximal end of the lateral trochlear ridge and one in the center of femoral diaphysis, in the most proximal end of the bone defect (Figures 6–8).

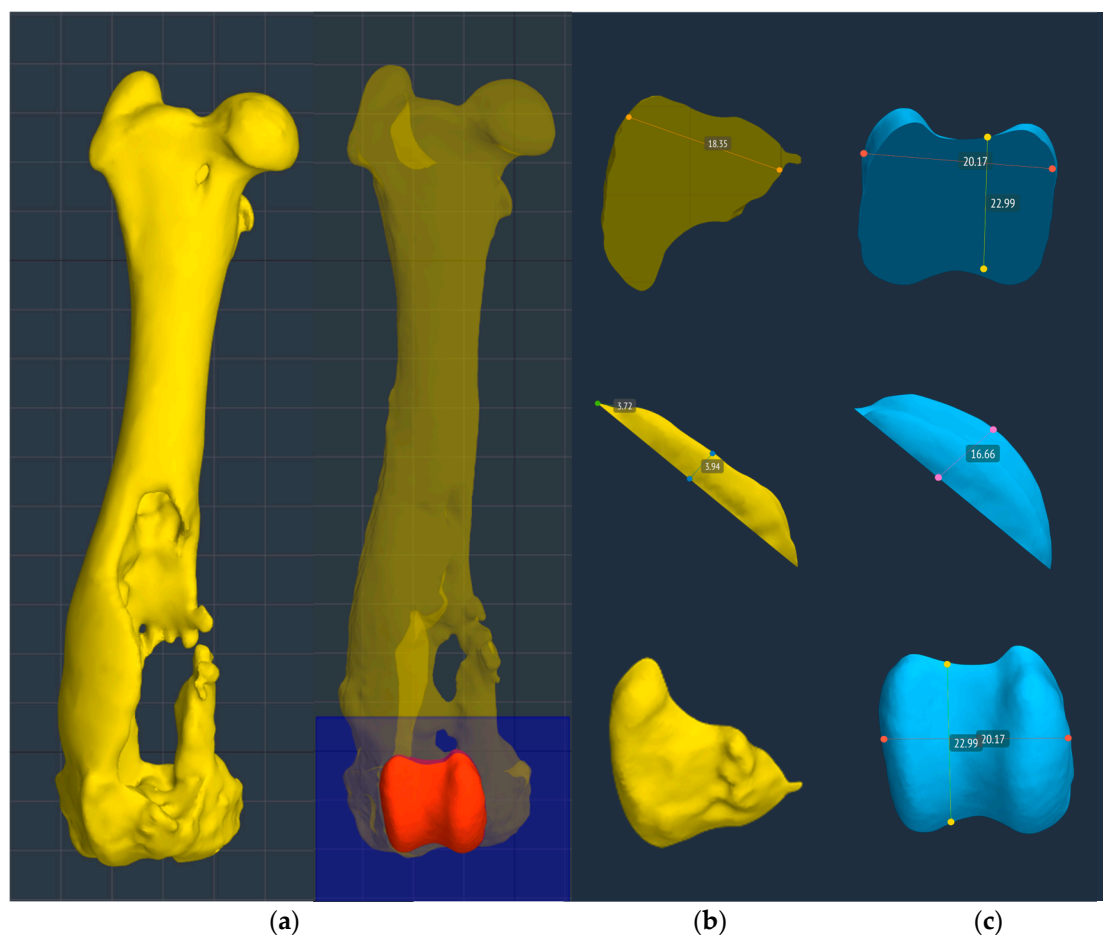


**Figure 6.** (a) The surface of the prosthesis that reproduced the femoral trochlea perfectly replicated the controlateral trochlea groove (red trochlea groove) and it was planned using BonaPlanner computer-aided design CAD software (Bonabyte LLC, Moscow). Reconstruction of the cranial surface (b) of the pathological distal femoral epiphysis with the partially intact lateral trochlear ridge and (c) of the controlateral distal femoral epiphysis, in particular of femoral trochlea.

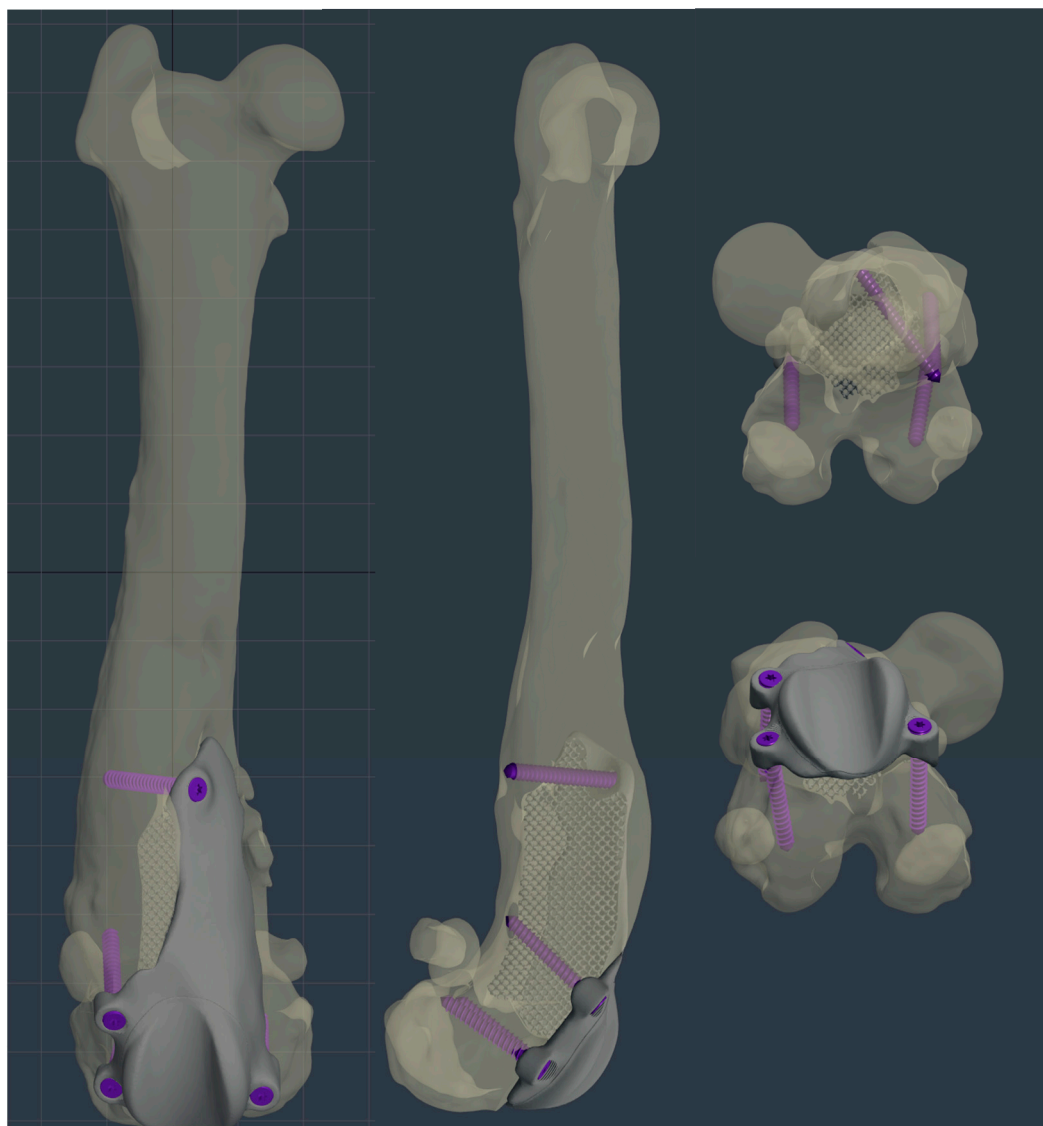


**Figure 7.** The custom-made PGR prosthesis was planned using BonaPlanner computer-aided design CAD software (Bonabyte LLC, Moscow). The prosthesis filled the bone defect and anatomically reproduced the shape of the femoral trochlea on the upper face of the implant. Four holes for screws was designed one laterally and one medially the distal margin of the lateral and medial trochlear ridges, one laterally the proximal end of the lateral trochlear ridge and one in the center of femoral diaphysis, in the most proximal end of the bone defect.

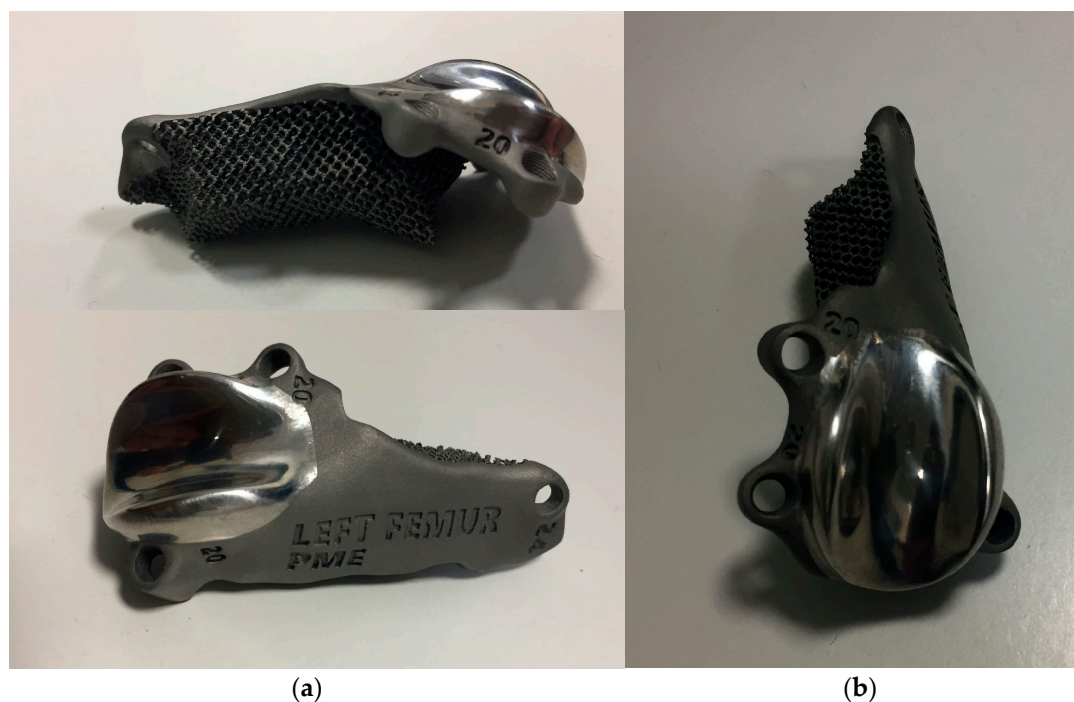


**Figure 8.** Photographs of (a) lateral (above), cranio-medial (below) and (b) cranial aspect of the custom-made PGR prosthesis. The implant was made of titanium Ti6Al4V ELI (grade 23) and the mirror surface of the prosthesis that reproduce the femoral trochlea was made by polishing with diamond base abrasive material made by hand. The portion of the prosthesis designed to fill the bone defect was completely porous to promote the bone growth and osteointegration.

### 2.3. Surgery

The dog was premedicated with methadone (0,2 mg/kg intramuscularly [IM]) and dexmedetomidine (1 µg/kg IM). General anesthesia was induced with propofol (2 mg/kg IV) and maintained with isoflurane in oxygen after endotracheal intubation. Loco-regional block with ropivacaine (1 mg/kg) of the sciatic and femoral nerves of the right hind limb was performed and constant rate infusion of fentanyl (5-20 µg/kg/h) was applied to provide analgesia. The antibiotic cefazolin (22 mg/kg IV) was administered one hour before surgery and repeated every 90 minutes until the end of the surgery.

The affected limb was aseptically prepared for surgery from the metatarsal-phalangeal joints to the coxo-femoral joint. The patient was positioned in dorsal recumbency and a lateral parapatellar approach was performed [22], prolonging the incision to the proximal end of the bone defect.

After reflection of the patella and the exposure of cranial surface of the distal femur, the debridement of the fibrous tissues from the cranial surface of the distal femoral metaphysis was performed using a pneumatic drill with diamond burs (Surgairtome two, Hall), in order to allow the placement of the osteotomy guide. Once the guide was properly positioned, the guide was fixed with four 2.0 mm Steinmann pins into the four designed holes. The osteotomy was performed with a motorized oscillating saw inserting the saw blade of 1 mm into the lateral slot in order to perform a lateral-medial osteotomy: the plan of osteotomy extended from the level of the origin of the tendon of the EDPL to the proximal end of the partially intact lateral trochlear ridge. The osteotomy guide was removed and the custom-made PGR prosthesis was applied. Once verified that the holes made for the application of the pins fit perfectly with the holes of the implant for the insertion of the screws, the custom-made PGR was stabilized to the bone with the four 2.7 mm titanium locking screws described previously (Figure 9).

The patella was reduced and tested in flexion and extension and an abundant lavage of the surgical field was performed. Capsulorrhaphy was executed with interrupted absorbable sutures and the subcutaneous tissues and skin were closed routinely.



**Figure 9.** The intraoperative image of the custom-made PGR stabilized to the bone.

### 2.3. Postoperative evaluation and management

Postoperative medio-lateral and caudo-cranial radiographs of the stifle joint were performed to evaluate the proper prosthesis position, the length of the screws and to confirm the patellar reduction (Figure 10). To improve the postoperative assessment, CT scans of the right stifle joint were obtained. A modified Robert-Jones splint was applied for 24 hours postoperatively. Meloxicam (0,1 mg/kg) once a day and amoxicillin and clavulanic acid (20 mg/kg) twice a day were prescribed for 10 days and only short walks on the leash to be gradually increased during the two months post-operative rehabilitation was recommended.

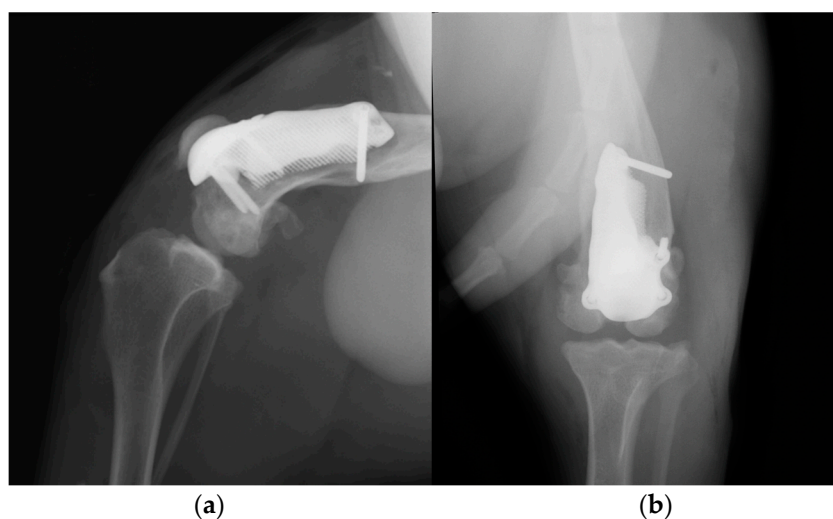


**Figure 10.** Postoperative medio-lateral (a) and caudo-cranial (b) radiographs of the stifle joint showed the appropriate prosthesis position, the correct length of the screws and the reduction of the patella.

A grade III of lameness (on scale from 0 to IV) [21] of the right hind limb was observed 24 hours postoperatively. Crepitus, mild pain and swelling of the right stifle joint were detected on manipulation, and the range of motion (ROM) was decreased due to the limited flexion and extension (Video S3a). The estimated angle of extension and flexion of the right stifle was 150-110° respectively and the thigh circumference was 28 cm.

Daily physiotherapy was started one day after the surgery. Massage of the hind limb and passive movement of right stifle joint, associated with instrumental therapies such as laser and tear were performed for 30 days in order to reduce inflammation and improve the joint excursion. Later, the active mobilization of the joint was also stimulated by an obstacle course and the physiotherapy was performed once a week for 6 months.

At the 3-month postoperative follow-up, an orthopedic, radiographic and tomographic examination were repeated. The patient showed a grade II right hindlimb lameness (Video S3b). On stifle joint palpation and manipulation, crepitus persisted. The arthralgia and capsular ectasia decreased compared to post-operative follow-up and mild pain was elicited at palpation of patellar ligament. The estimated angle of extension and flexion of the right stifle was 150-90° respectively. The radiographic and tomographic evaluations revealed absence of implant associated complication, such as implant loosening and migration, and a thickening of the patellar ligament, sign of suspicious desmitis (Figure 11).

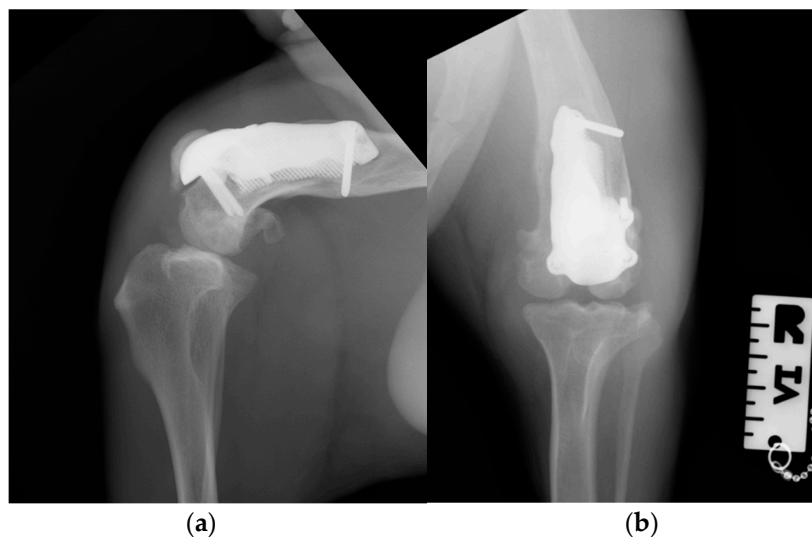


**Figure 11.** Three-month postoperative medio-lateral (a) and caudo-cranial (b) radiographs of stifle joint showed absence of implant-associated complication, such as implant loosening and migration, and a thickening of the patellar ligament and sign of suspicious desmitis.

At the 6, 12 and 18-month follow-up (Video S3c), the orthopedic evaluation revealed crepitus, but a grade 0 right limb lameness, absence of patellar ligament desmitis and palpation of the right stifle joint did not elicit pain. The estimated angle of extension and flexion of the right stifle was 160-80° respectively, while the ROM of the contralateral healthy limb was 160° in extension and 40° in flexion. The thigh circumference of the pathologic limb was 40 cm compared with 47 cm of the healthy one. The radiographic images showed a good osseointegration of the implant (Figure 12).

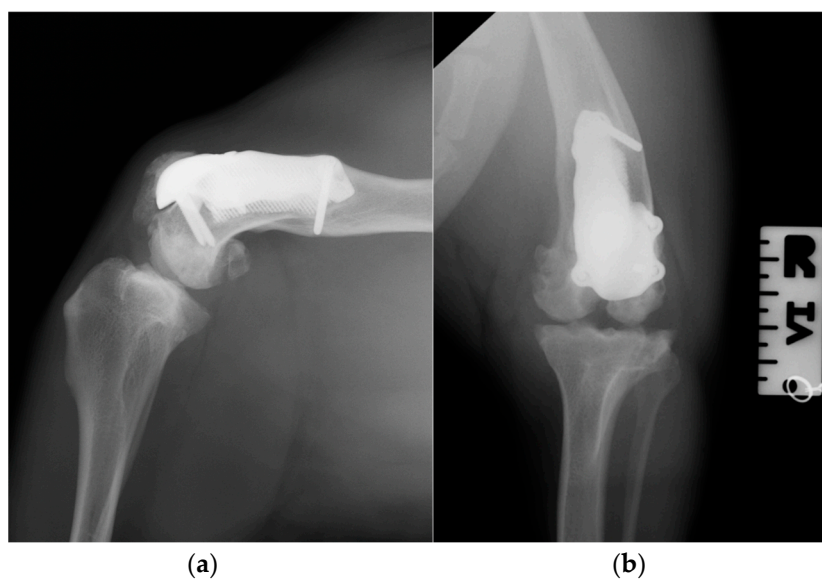


**Figure 12.** Twelve-month postoperative medio-lateral (a) and caudo-cranial (b) radiographs of stifle joint showed a good osteointegration of the implant.

#### 4. Discussion

This report describes the use of a custom-made PGR prosthesis to treat an extensive bone defect and to restore the articular surface of the femoral trochlea in an American Staffordshire terrier puppy, affected by a severe hematogenous osteomyelitis of the metaphysis and of the distal-middle third of the right femoral diaphysis.

To our knowledge, this is the first report on custom-made PGR available in the literature [12,16,23]. Despite the serious injury that afflicted the right pelvic limb, the surgery had satisfactory outcomes until the last 18-months postoperative follow up. The patient fully resumed the functionality of the pelvic limb and no major complications were detected [24]. The only complication detected was the patellar ligament desmitis revealed at the 3-month postoperative follow-up. This minor complication was managed by controlled physical exercise and physiotherapy, without administration of additional drugs [24]. This complication was expected because for four months (time elapsed from the first visit at 8 months of age, to prosthetic surgery, at 12 months of age) the soft tissues adapted to a deformed and incomplete femoral trochlea leading to failure of the stifle extensor mechanism [25]. The application of the custom-made PGR prosthesis and the reduction of the patella might have determined an increased strain of the patellar ligament, which is a cause of development of ligament desmitis [26].

The complete resorption of the cranio-medial cortex of the distal femur with involvement of the femoral trochlea and the presence of a bone defect represent a complex orthopedic condition to face. The use of standard PGR to restore the femoral trochlea surface was precluded because of loss of bone surface to apply the implant [16], so it was decided to design a custom-made prosthesis using 3D-printing technologies. The implementation of these innovative surgical techniques has enabled the management of highly complex situations that were previously only addressed through salvage procedures, such as arthrodesis or amputations [12,27–29]. In veterinary practice, despite the growing interest, the application of 3D-printing technologies is in the early stage [30–32]. To date, the 3D printing in veterinary orthopedics is used for the manufacturing of anatomical models (for preoperative planning and surgical rehearsal, education, communication), of medical device (such as custom-made plate, saw or drill guide, implants and prosthesis) and of tissue engineering (such as custom-designed scaffold and surface coating for osseointegration [12]).

The custom-made PGR had several advantages. Firstly, the component of the prosthesis designed to fill the bone defect was completely porous for long-term biologic fixation, promoting the bone growth and osseointegration [16,27]. Secondly, the prosthesis completely removes the bone defect, which could be a site of bacterial colonization resulting in recurrent infections [6]. Thirdly, the upper face of the implant anatomically reproduces the shape of the contralateral femoral trochlea, allowing the repositioning of the patella, preventing its dislocation, and restoring the function of the patella-femoral joint. In addition, the surface of the prosthesis that reproduce the femoral trochlea was treated with amorphous diamond base coating to reduce the coefficient of friction [16]. Last but not least, four holes for screws were designed to secure the custom-made PGR to the bone despite the alteration of the anatomy of distal femur. The rationale for the screw position was to bridge the defect and to fix the prosthesis immediately.

The custom-made PGR was manufactured with the titanium alloy, a common alloy used in biomedical components, highly biocompatible and corrosion resistant like the pure titanium, but with a superior fatigue resistance [33,34]. In particular we used the Ti-6Al-4V ELI, an alloy where the interstitial elements such as oxygen, carbon, and iron are deliberately kept low in order to improved fracture toughness and ductility [35].

The high cost of the implant and the complexity of the manufacturing are disadvantages of the use of a custom-made PGR. In addition, the prosthetic surgery was performed once the dog had completed skeletal growth because the custom-made implants are not suitable for growing dogs: the prosthesis does not subsequently adapt to the growth of the patient leading to possible implant failure. Another disadvantage of a custom-made implant is that usually requires the realization of cutting guides where it is necessary to perform osteotomies for the placement of the prosthesis [36]. The cutting guides improve the surgical precision [12], but they require a proper fit on the bone

structure and a precise and stable placement [36–38]. In our report, major point for the correct execution of the surgery was in fact the debridement of the fibrous tissues from the cranial surface of the distal femoral metaphysis, in order to allow the proper placement of the osteotomy guide, and the fixation of the guide with Steinmann pins. The fibrous tissues and adhesions that developed during these months were abundant and difficult to remove, so it was decided to use an high speed bur and a surgical electric cutter to obtain a better debridement. For surgical application of the PGR commercially available, the cut of the trochlea is performed in free-hand fashion following anatomical landmarks established [16]. A strong point in our case report is the use of the cutting guide, designed for the specific patient. It was planned to fix the guide to the bone by means of four 2.0 mm Steinmann pins. The holes of the pins of the guide will correspond with the holes for the screws of the prosthesis, in order to have a perfect spatial positioning of the PGR consistent with the pre-operative planning and without risk of recurrent patellar luxation or malalignment.

In this case report, the use of the custom-made implant has become indispensable for the treatment of severe bone lesions secondary to osteomyelitis. Osteomyelitis is an infectious condition that affects the bone, causing progressive inflammation which leads to destruction of bone tissue and the formation of new bone [1,10]. The management of osteomyelitis entails the administration of a prolonged antibiotic therapy and the debridement or resection of infected and necrotic bone, depending on the severity and extent of the infectious process [6,11]. This therapeutic approach aims to eradicate the infected tissue and facilitate osseous healing [6,11]. In our patient, a persisting bone sequestrum perpetuated the infection, manifesting as recurrent fever that exhibited only partial responsiveness to systemic antibiotic therapy. A month has elapsed between the onset of osteomyelitis and bone sequestrum removal, and this period of latency was responsible for severe articular impairment characterized by trochlear cartilage and subchondral bone destruction. The excision of the sequestrum, followed by targeted antibiotic therapy, effectively eradicated the infection both locally and systemically. Subsequently, after one month, a grade IV lameness persisted in the affected limb, but the absence of systemic symptoms indicative of infection, such as hyperthermia, lethargy and inappetence, was observed in the patient. Considering the young age of our patient, the anamnesis of endocarditis and absence of a traumatic event, and the metaphyseal location of the osteomyelitis, there was a strong suspicion of hematogenous osteomyelitis [1,6]. In human medicine, the incidence of vertebral osteomyelitis is high in patients with infective endocarditis [39], but this correlation between osteomyelitis and endocarditis was not revealed in veterinary medicine.

*Staphylococcus* spp. is the predominant bacteria detected in approximately 60% of osteomyelitis cases in dogs and cats, with *Escherichia coli* and *Streptococcus* spp. Additionally, other Gram-negative microorganisms such as *Pasteurella*, *Pseudomonas*, *Proteus*, *Serratia*, and *Klebsiella* species, as well as Gram-positive organisms like *Corynebacterium* spp. and enterococci, have also been isolated [1,3,40]. In our patient, *Klebsiella oxytoca* was isolated in the synovial liquid and in the in adjacent bone tissue. It is not a single species but a complex comprising at least six species, i.e., *Klebsiella grimontii*, *Klebsiella huaxiensis*, *Klebsiella michiganensis*, *K. oxytoca*, *Klebsiella pasteurii*, and *Klebsiella spallanzanii* [41]. In humans, *K. oxytoca* is a member of the normal gut microflora, but is also an important human pathogen causing a large variety of infections ranging from mild diarrhea to life-threatening bacteremia, meningitis [41,42] and endocarditis [43]. In literature, there is a paucity of reports that describe *Klebsiella oxytoca* infection in dogs [44].

Limitations of this report include the fact that it was based on a single case, even though it showed excellent short-, medium- and long-term outcomes [24]. Furthermore, postoperative complications such as aseptic loosening and mechanical failure of the implant may not become evident during follow-up until 18 months after the surgery.

## 5. Conclusions

To the best of our knowledge, this is the first report which describes the use of a custom-made PGR prosthesis. Based on the clinical, radiographic and tomographic outcomes, the use of a custom-made PGR prosthesis was an effective treatment to restore the articular surface of the femoral trochlea and resolve the bone defect.

**Supplementary Materials:** Video S1: The patient manifested lethargy, inappetence and anorexia and no weightbearing lameness and severe edema of the right hind limb were revealed. Video S2: At 12 months of age, the patient manifested a grade III of lameness, significant muscle hypotrophy, pain on manipulation of the right stifle, joint swelling and grade III medial patellar luxation. The severe edema of the limb observed during the first orthopedic evaluation disappeared. Video S3: (a) At one-day postoperative follow-up the patient revealed a grade III right limb lameness [21]. During the following follow up at (b) 3-month and (c) 18-month, the lameness of the right limb decreased from a grade II to a 0 [21], respectively.

**Author Contributions:** Conceptualization, E.P. and A.P.P.; methodology, E.P. and G.M.C.; software C.B., M.B., E.B. and F.C.; validation, E.P.; investigation, V.R.; resources, C.B. and S.S.; data curation, G.M.C., C.B. and S.S.; writing—original draft preparation S.S.; writing—review and editing, S.S. and A.P.P.; visualization, E.P., C.B. and S.S.; supervision, A.P.P.; project administration, E.P. and A.P.P. All authors have read and agreed to the published version of the manuscript.

**Funding:** This research received no external funding.

**Institutional Review Board Statement:** Ethical review and approval were waived for this study due to the fact that it is a case report of a surgery performed for the purpose of treatment of patient, necessary to ensure the patient's well-being and recovery, and no action contrary to treatment was performed.

**Informed Consent Statement:** Not applicable.

**Data Availability Statement:** The data present in this study are available within the article.

**Conflicts of Interest:** The authors declare no conflict of interest.

## References

1. Robinson, D.: Osteomyelitis and Implant-Associated Infections. In *Veterinary Surgery Small Animal*, 2th ed.; Johnston, S.A., Tobias, K.M., Eds.; Elsevier Saunders: St. Louis, MO, USA, 2018; 47, pp. 669-675. [[CrossRef](#)][[PubMed](#)]
2. Weisbrode, S.E. Knochen und Gelenke. *Pathologie der Haustiere: Allgemeine, spezielle und funktionelle Veterinärpathologie*; McGavin, M.D., Zachary, J.F., Eds.; Urban and Fischer in Elsevier, München, GER, 2009; pp. 966.
3. Johnson, K.A. Osteomyelitis in dogs and cats. *J. Am. Vet. Med. Assoc.* **1994**, *204*, 1882–1887. [[PubMed](#)]
4. Pacchiana, P.D.; Morris, E.; Gillings, S.L.; Jessen, C.R.; Lipowitz, A.J. Surgical and postoperative complications associated with tibial plateau leveling osteotomy in dogs with cranial cruciate ligament rupture: 397 cases (1998-2001). *J. Am. Vet. Med. Assoc.*, **2003**, *222*, 184–193. [[PubMed](#)]
5. Panichi, E.; Cappellari, F.; Peirone, B.; Piras, L. Treatment of antebrachial and crural septic nonunion fractures in dogs using circular external skeletal fixation: a retrospective study. *Vet. Comp. Orthop. Traumatol.* **2014**, *27*, 297-305. [[CrossRef](#)][[PubMed](#)]
6. Gieling, F.; Peters, S.; Erichsen, C.R.; Richards, G.; Zeiter, S.T.; Moriarty, F. Bacterial osteomyelitis in veterinary orthopaedics: pathophysiology, clinical presentation and advances in treatment across multiple species. *Vet. J.* **2019**, *250*, 44–54. [[CrossRef](#)][[PubMed](#)]
7. Greene, C.E., Bennett, D. Musculoskeletal infections. In *Infectious diseases of the dog and cat*, 4th ed.; Greene, C.E., Eds.; Elsevier Saunders: St Louis, MO, USA, 2012; pp. 892–912.
8. Trueta, J. The three types of acute haematogenous osteomyelitis: A clinical and vascular study. *J. Bone Joint Surg. Br.*, **1959**, *41*, 671–680. [[PubMed](#)]
9. Lew, D.P., Waldvogel, F.A. Osteomyelitis. *The Lancet*, **2004**, *364*, 369–379. [[CrossRef](#)][[PubMed](#)]
10. Thrall, D.E. Radiographic Features of Bone Tumors and Bone Infections in Dogs and Cats. In *Textbook of Veterinary Diagnostic Radiology*, 7th ed.; Thrall, D.E., Eds.; Elsevier Saunders: St. Louis, MO, USA, 2018; 20, pp. 390-402.

11. Glass, K., Watts, A.E. Septic arthritis, physitis, and osteomyelitis in foals. *Vet. Clin. Equine* **2017**, *33*, 299–314. [[CrossRef](#)][[PubMed](#)]
12. Memarian, P., Pishavar, E., Zanotti, F., Trentini, M., Camponogara, F., Soliani, E., Gargiulo, P., Isola, M., Zavan, B. Active materials for 3D printing in small animals: current modalities and future directions for orthopedic applications. *Int. J. Mol. Sci.* **2022**, *23*, 1045. [[CrossRef](#)][[PubMed](#)]
13. Bruecker, K.A., Benjamino, K., Vezzoni, A., Walls, C., Wendelburg, K.L., Follette, C.M., Déjardin, L.M., Guillou, R. Canine elbow dysplasia. Medial compartment disease and osteoarthritis. *Vet. Clin. Small Anim.* **2021**, *51*, 475–515. [[CrossRef](#)][[PubMed](#)]
14. Peck, J.N.; Marcellin-Little, D.J. *Advances in Small Animal Total Joint Replacement*; John Wiley & Sons: Hoboken, NJ, USA, 2012; Volume 4, ISBN 9780470959619.
15. Allen, M.J. Advances in total joint replacement in small animals. *J. Small Anim. Pract.* **2012**, *53*, 495-506. [[CrossRef](#)][[PubMed](#)]
16. Dokic, Z.; Lorinson, D.; Weigel, J.P.; Vezzoni, A. Patellar groove replacement in patellar Luxation with severe femoro-patellar osteoarthritis. *Vet. Comp. Orthop. Traumatol.* **2015**, *28*, 124–130. [[CrossRef](#)][[PubMed](#)]
17. Hoang, D., Perrault, D., Stevanovic, M., Ghiassi, A. Surgical applications of three-dimensional printing: a review of the current literature & how to get started. *J. Transl. Med.*, **2016**, *4*, 456-456. [[CrossRef](#)][[PubMed](#)]
18. Schmierer, P.A. & Böttcher, P. Patient specific, synthetic, partial unipolar resurfacing of a large talar osteochondritis dissecans lesion in a dog. *Vet. Surg.* **2023**, *52*, 731–738. [[CrossRef](#)][[PubMed](#)]
19. Singleton, W.B. The surgical correction of stifle deformities in the dog. *J. Small Anim. Pract.* **1969**, *10*, 59. [[CrossRef](#)][[PubMed](#)]
20. Innes, J. Arthritis. In *Veterinary Surgery Small Animal*, 2th ed.; Johnston, S.A., Tobias, K.M., Eds.; Elsevier Saunders: St. Louis, MO, USA, 2018; 68: 1078-1111.
21. Vasseur, P.B.; Johnson, A.L.; Budsberg, S.C.; Lincoln, J.D.; Toombs, J.P.; Whitehair, J.G.; Lents, E.L. Randomized controlled trial of the efficacy of carprofen, a nonsteroidal anti-inflammatory drug, in the treatment of osteoarthritis in dogs. *J. Am. Vet. Med. Assoc.* 1995, *206*, 807–811. [[PubMed](#)]
22. Johnson, K.A. Piermattei's Atlas of Surgical Approaches to the Bones and Joints of the Dog and Cat. In *Piermattei's Atlas of Surgical Approaches to the Bones and Joints of the Dog and Cat*, 5th ed.; Johnson, K. A., Eds.; Elsevier Saunders: St. Louis, MO, USA, 2014; 7, 367–460.
23. Kim, Y.; Park, Y.; Park, J.; Jeong, S.M.; Lee, H. Bilateral patellar groove replacement in a dog with iatrogenic trochlear groove damage. *J. Vet. Clin.* **2016**, *33*, 295–299. [[CrossRef](#)]
24. Cook, J.L.; Evans, R.; Conzemius, M.G.; Lascelles, B.D.x; McIlwraith, C.W.; Pozzi, A.; Clegg, P.; Innes, J.; Schulz, K.; Houlton, J.; Fortier, L.; Cross, A.R.; Hayashi, K.; Kapatkin, A.; Brown, D.C.; Stewart, A. Proposed definitions and criteria for reporting time frame, outcome, and complications for clinical orthopedic studies in veterinary medicine. *Vet. Surg.* **2010**, *39*, 905-908. [[CrossRef](#)][[PubMed](#)]
25. Perry, K.L., Déjardin, L.M. Canine medial patellar luxation. *J. Small Anim. Pract.* **2021**, *62*, 315-335. [[CrossRef](#)][[PubMed](#)]
26. Mattern, K.; Clifford, R.B; Jeffrey, N.P; Jacek, J.D. Radiographic and ultrasonographic evaluation of the patellar ligament following tibial plateau leveling osteotomy. *Vet. Radiol. Ultrasound* **2006**, *47*, 185–191. [[CrossRef](#)][[PubMed](#)]
27. Castelli, E.; Schmierer, P.A.; Pozzi, A. Custom acetabular prosthesis for total hip replacement: A case report in a dog with acetabular bone loss after femoral head and neck ostectomy. *Vet. Surg.* **2019**, *48*, 1520–1529. [[CrossRef](#)][[PubMed](#)]
28. Nojiri, A.; Akiyoshi, H.; Ohashi, F.; Atsuki, I.; Sawase, O.; Matsushita, T.; Takemoto, M.; Fujibayashi, S.; Nakamura, T.; Yamaguchi, T. Treatment of a unicameral bone cyst in a dog using a customized titanium device. *Vet. Med. Sci.* **2015**, *77*, 127–131. [[CrossRef](#)][[PubMed](#)]
29. Liska, W.D.; Marcellin-Little, D.J.; Eskelinen, E.V.; Sidebotham, C.G.; Harrysson, O.L.A.; Hielm-Bjorkman, A.K. Custom total knee replacement in a dog with femoral condylar bone loss. *Vet. Surg.* **2007**, *36*, 293–301. [[CrossRef](#)][[PubMed](#)]
30. Hespel, A.M.; Wilhite, R.; Hudson, J. Invited review-applications for 3D printers in veterinary medicine. *Vet. Radiol. Ultrasound* **2014**, *55*, 347–358. [[CrossRef](#)][[PubMed](#)]
31. Popov, V.V.; Muller-Kamskii, G.; Katz-Demyanetz, A.; Kovalevsky, A.; Usov, S.; Trofimcow, D.; Dzhenzhera, G.; Koptuyug, A. Additive manufacturing to veterinary practice: Recovery of bony defects after the osteosarcoma resection in canines. *Biomed. Eng. Lett.* **2019**, *9*, 97–108. [[CrossRef](#)][[PubMed](#)]

32. Harrysson, O.L.A.; Marcellin-Little, D.J.; Horn, T.J. Applications of Metal Additive Manufacturing in Veterinary Orthopedic Surgery. *JOM* 2015, 67, 647–654. [[CrossRef](#)]
33. Veiga, C.; Davim, J.P.; Loureiro, A.J.R. Properties and applications of titanium alloys: A brief review. *Rev. Adv. Mater. Sci.* 2012, 32, 133–148.
34. Elsayed, H.; Rebesan, P.; Giacomello, G.; Pasetto, M.; Gardin, C.; Ferroni, L.; Zavan, B.; Biasetto, L. Direct ink writing of porous titanium (Ti6Al4V) lattice structures. *Mater. Sci. Eng. C.* 2019, 103, 109794. [[CrossRef](#)][[PubMed](#)]
35. Yan, X.; Yin, S.; Chen, C.; Huang, C.; Bolot, R.; Lupoi, R.; Kuang, M.; Ma, W.; Coddet, C.; Liao, H.; et al. Effect of heat treatment on the phase transformation and mechanical properties of Ti6Al4V fabricated by selective laser melting. *J. Alloys Compd.* 2018, 764, 1056–1071. [[CrossRef](#)]
36. Nicetto, T.; Longo, F. Trochlear ridge prostheses for reshaping femoral trochlear ridges in dogs with patellar luxation. *Vet. Comp. Orthop. Traumatol.* 2023. [[CrossRef](#)][[PubMed](#)]
37. Lee, H.R.; Adam, G.O.; Yang, D.K.; Tungalag, T.; Lee, S.J.; Kim, J.S.; Kang, H.S.; Kim, S.J.; Kim, N.S. An easy and economical way to produce a three-dimensional bone phantom in a dog with antebrachial deformities. *Animals* 2020, 10, 1445. [[CrossRef](#)][[PubMed](#)]
38. Worth, A.J.; Crosse, K.R.; Kersley, A. Computer-Assisted Surgery Using 3D Printed Saw Guides for Acute Correction of Antebrachial Angular Limb Deformities in Dogs. *Vet. Comp. Orthop. Traumatol.* 2019, 32, 241–249. [[CrossRef](#)][[PubMed](#)]
39. Tamura, K. Clinical characteristics of infective endocarditis with vertebral osteomyelitis. *J. Infect. Chemother.* 2010, 16, 260–265. [[CrossRef](#)][[PubMed](#)]
40. Siqueira, E.G.; Rahal, S.C.; Ribeiro, M.G.; Paes, A.C.; Listoni, F.P.; Vassallo, F.G. Exogenous bacterial osteomyelitis in 52 dogs: A retrospective study of etiology and in vitro antimicrobial susceptibility profile (2000–2013). *Vet. Q.* 2014, 34, 201–204. [[CrossRef](#)][[PubMed](#)]
41. Yang, J.; Long, H.; Hu, T.; Feng, Y.; McNally, A.; Zonga, Z. *Klebsiella oxytoca* complex: Update on taxonomy, antimicrobial resistance, and virulence. *Clin. Microbiol. Rev.* 2022, 35, e0000621. [[CrossRef](#)][[PubMed](#)]
42. Hogenauer, C.; Langner, C.; Beubler, E.; Lippe, I.T.; Schicho, R.; Gorkiewicz, G.; Krause, R.; Gerstgrasser, N.; Krejs, G.J.; Hinterleitner, T.A. *Klebsiella oxytoca* as a causative organism of antibiotic-associated hemorrhagic colitis. *N. Engl. J. Med.* 2006, 355, 2418–2426. [[CrossRef](#)][[PubMed](#)]
43. Aissaoui, H.; Hdidou, T.; Bougrine, R.; Ismaili, N.; El ouafi, N. Infective endocarditis caused by *Klebsiella oxytoca* in a patient with hemodialysis: a CARE-compliant case report and review of the literature. *J. Saudi Heart Assoc.* 2020, 32, 307–310. [[CrossRef](#)][[PubMed](#)]
44. Seliškar, A.; Zdovc, I.; Zorko, B. Nosocomial *Klebsiella oxytoca* infection in two dogs. *Slov. Vet. Res.* 2007, 44, 115–122. [[CrossRef](#)]

**Disclaimer/Publisher's Note:** The statements, opinions and data contained in all publications are solely those of the individual author(s) and contributor(s) and not of MDPI and/or the editor(s). MDPI and/or the editor(s) disclaim responsibility for any injury to people or property resulting from any ideas, methods, instructions or products referred to in the content.